Improved Control of Current Controlled Grid Connected Inverters in Adjustable Speed Power Energies

J.J. Vague Cardona[1], J.C. Alfonso Gil[2], F.J. Gimeno Sales[3], S. Segui-Chilet[4], S. Orts Grau[5], N. Muñoz Galeano[6]

[1-5] Department of Electronics Engineering
(I.Q.M.A.), Universidad Politécnica de Valencia
Campus of Vera – Camino de Vera s/n, 46022 Valencia (Spain)
Phone:+0034 963 876076, e-mail: jvague@dcom.upv.es, joalgi2@etsii.upv.es, fjgimeno@eln.upv.es, ssegui@eln.upv.es, sorts@eln.upv.es

[6]Department of Electrical Engineering
Universidad de Antioquia
Calle 63, Número 53-108, Medellin (Colombia)
e-mail: nicolasm@udea.edu.co

Abstract. This Paper presents a comparison of two control strategies applied to current controlled inverters in renewable energy systems. The strategies are the Synchronous Reference Frame and Stationary Reference Frame. First control method use PI regulators and it is the most used inverters control. In this paper, it is shown how to simplify the parameters design of the Proportional-Resonant controller for the Stationary Reference Frame. This paper presents the grid model and detailed design and stability analysis with a modified Symmetry Criterion method for the PI regulator parameters calculus. From this point, we transform the designed PI regulator into a PR, which it's needed for the Stationary Reference Frame Control. Results in terms of THD_i indicate the better performance of PR control.

Key words
Synchronous Frame, Stationary Frame, Resonant Controllers, Voltage Oriented Control, Voltage Source Inverters, Symmetry Criterion.

1. Introduction

Nowadays, Wind Turbine Systems Generators (WTSG) with Direct-Drive Permanent Magnet Generator (DDPMG) is one of the preferred technologies in variable speed. Wind turbine usually rotates at the speed of 30-50 rev/min, and generators should rotate at 1000-1500 rev/min to interface directly with the grid. Usually, a gear box should be connected between wind turbine and the electric generator. Direct connection of the generator to the wind turbine requires a large number of poles. Permanent Magnet Synchronous Generators (PMSG) are the best choice to be used, with a small pole pitch and cost-effective design [1].

Wind turbine system is known to have a slow response, this kind of systems are suitable for grid connection applications in which the dynamics requirement can be demanded by a slow current ramp. We have to manage the extracted energy from WTSG to the grid via a fully scale Back-to-Back converters. Generator side converter aims to control the output power from the DDPMG thanks to Maximum Power Point Tracking algorithm.

Power flow is balanced via the DC link to the Grid Side Power Electronic Converter. It aims to maintain the DC-Bus voltage and translates the generated energy to the grid through its inductance filter. As the inductor is made smaller it improves the ability to track the desired reference current, however we have to increase the switching frequency to reduce current line ripple [2][3].

In this paper, PI regulator parameters are calculated in the Synchronous Reference Frame. This method is based on voltage space-vector oriented reference frame, also called Voltage Oriented Control (VOC) [4]. Then, Power is controlled thanks to the current regulators, which are the control mode of our Voltage Source Inverter (VSI).

Classical PI regulators are unsatisfactory for Stationary Reference Frame (AC control). We have to use a Proportional-Resonant controller to resolve the problem. Resonant Controllers don't have to transform a measured stationary frame ac current to rotating frame dc quantities. If transformation is not accurate errors could be introduced at the synchronous compensation network. Stationary frame controller is obtained using the transfer function proposed in [5].

Control scheme has been implemented using Matlab Simulink®. Paper presents the comparison results from the point of view of the harmonic content of injected currents (THDi).

2. Synchronous Reference Frame Control.

The proposed system is a three-phase inverter connected to grid. Figure 1 show the electrical schematic, where the reactance is connected between the electronic IGBT-Bridge and the Grid. Source Power is a WTSG with PMSG. We consider Bus-DC an ideal voltage DC source. This paper is not focused in the PMSG control but in the Grid-Side converter control.

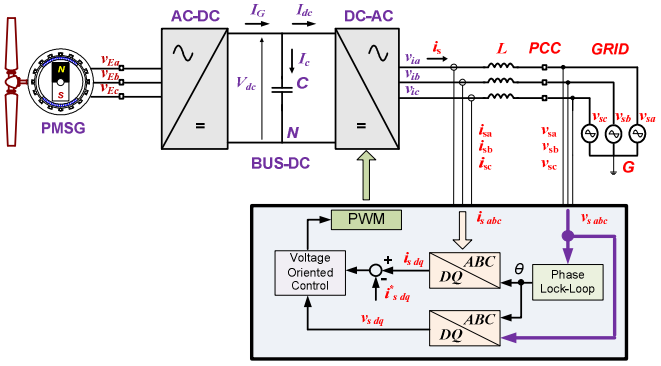

Fig. 1. Grid Connection with L-Filter

In Figure 1 voltages and currents can be written as:

$$v_{ik} = R \cdot i_{sk} + L \cdot \frac{d}{dt} i_{sk} + v_{sk} + v_{NG}, \quad k = a,b,c \tag{1}$$

Where v_{ik} is the inverter voltage output, v_{sk} is the grid voltage, and R-L are the values of the reactance or L-Filter and v_{NG} is the voltage between ground and negative of DC-Bus. In the conventional three phase inverter with balanced load and without fourth wire neutral v_{NG} is always zero [6].

Representing (1) in a space-vector with α-axis over phase a stationary reference frame [2]:

$$v_{i\alpha\beta} = R \cdot i_{s\alpha\beta} + L \frac{di_{s\alpha\beta}}{dt} + v_{s\alpha\beta} \tag{2}$$

Where $i_{s\_\alpha\beta}$ is the current in the α-β plane, $v_{i\_\alpha\beta}$ is the inverter output voltage and $v_{s\_\alpha\beta}$ is the grid voltage.

In the synchronous reference frame with angular speed ω_s (d-axis synchronized with grid voltage vector) equations are [2]:

$$v_{idq} = R \cdot i_{sdq} + L \frac{di_{sdq}}{dt} - jL\omega \cdot i_{sdq} + v_{sdq} \tag{3}$$

VOC works in the voltage space-vector reference frame. Direct axis lies in the direction of the grid voltage space vector. We could represent this equation in its direct axis "d" and its quadrature axis "q":

$$v_{s\_dq} = v_{sd} + jv_{sq}$$

$$v_{sq} = 0 \begin{cases} v_{id} = R \cdot i_{sd} + L \frac{di_{sd}}{dt} + L\omega_s \cdot i_{sq} + v_{sd} \\ v_{iq} = R \cdot i_{sq} + L \frac{di_{sq}}{dt} - L\omega_s \cdot i_{sd} + v_{sq} \end{cases} \tag{4}$$

At the Point of Common Coupling (PCC) grid voltage v_s doesn't have quadrature component:

$$\begin{aligned} v_{id} &= R \cdot i_{sd} + L \frac{di_{sd}}{dt} + L\omega_s \cdot i_{sq} + v_{sd} \\ v_{id} &= R \cdot i_{sd} + L \frac{di_{sd}}{dt} + v_{coupling\ d} + v_{sd} \end{aligned} \tag{5}$$

$$\begin{aligned} v_{iq} &= R \cdot i_{sq} + L \frac{di_{sq}}{dt} - L\omega_s \cdot i_{sd} \\ v_{iq} &= R \cdot i_{sq} + L \frac{di_{sq}}{dt} - v_{coupling\ q} \end{aligned} \tag{6}$$

Then, in a linear and symmetric three-phase system active and reactive power is reduced to control d-axis and q-axis currents (v_{sq}=0):

$$P = \frac{3}{2}\left(v_{sd}i_{sd} + v_{sq}i_{sq}\right) \rightarrow P = \frac{3}{2}\left(v_{sd}i_{sd}\right) \tag{7}$$

$$Q = \frac{3}{2}\left(v_{sq}i_{sd} - v_{sd}i_{sq}\right) \rightarrow Q = -\frac{3}{2}\left(v_{sd}i_{sq}\right) \tag{8}$$

The control inputs in (5) and (6) are v_{id} and v_{iq}, while v_{sd} could be seen as a disturbance to be measure.

3. VOC model disturbances.

Disturbances in (5) and (6) are the grid-voltage and cross-coupling terms. Large signal equations can be derived using duty-cycle averaging. Then, inverter output voltage could be expressed [6]:

$$v_{ik} = d_{ik} \cdot G_{PWM} \xrightarrow{dq} \vec{v}_{i\,dq} = \vec{d}_{i\,dq} \cdot G_{PWM} \tag{9}$$

Where, G_{PWM} is the non-linear PWM modulator gain [6],[7]. At the Synchronous Frame, Cross-Coupling terms are given by:

$$v_{coupling\ dq} = jL\varpi \cdot i_{s\,dq} \begin{cases} v_{coupling\ d} = L\omega_s \cdot i_{sq} \\ v_{coupling\ q} = -L\omega_s \cdot i_{sd} \end{cases} \tag{10}$$

Taking (9) into account, (5) and (6) can be transformed in:

$$\begin{aligned} G_{PWM}\left(d_{id} + \frac{v_{coupling\,d}}{G_{PWM}} - \frac{v_{sd}}{G_{PWM}}\right) &= R \cdot i_{sd} + L\frac{di_{sd}}{dt} \\ G_{PWM}\left(d_{iq} + \frac{v_{coupling\,q}}{G_{PWM}} - \frac{v_{sq}}{G_{PWM}}\right) &= R \cdot i_{sq} + L\frac{di_{sq}}{dt} \end{aligned} \tag{11}$$

Current Cross-Coupling and grid-voltage terms should be *compensated* with "Feed-Forward" them. At that point, we can use classical techniques of regulator design. Then, *compensating terms* can be written as:

$$v_{compd} = \frac{v_{sd} - v_{cpl\,d}}{G_{PWM}} \tag{12}$$

$$v_{comp\,q} = \frac{v_{sq} - v_{cpl\,q}}{G_{PWM}} \tag{13}$$

Figure 2 shows the power converter control scheme. In the synchronous frame PI regulators can achieve zero steady-state error by acting on current control signals. Feed-Forward terms are introduced in this Block-Diagram.

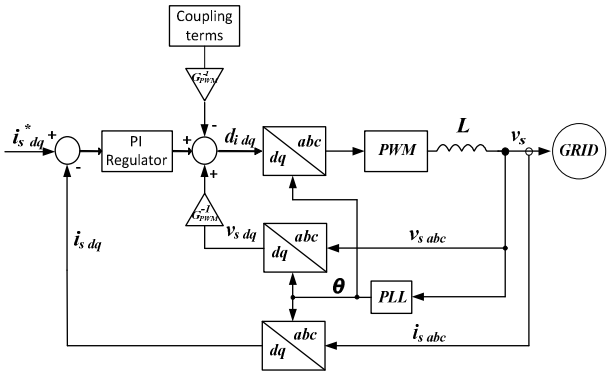

Fig. 2. Inverter VOC control scheme.

Note that G_{PWM} gain is also feed-forward in form of block $1/G_{PWM}$ and it takes V_{dc} value into account. Finally, a saturable block (which is not represented in Figure 2) is used between abc to dq block and PWM module. Thanks to this block we work in the linear range of the modulator.

4. VOC Current Loop Design.

A feed-back control system is as shown in Figure 3, where output current I_s is measured and compared with a reference value. Signal *d(s)* is the average value of switching signals in the Laplace domain. To optimize closed loop response we need the open loop transfer function.

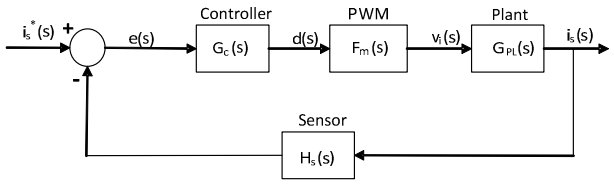

Fig. 3. Control Feed-back block-diagram.

Open Loop Transfer Function (*TF*) with sensor $H_s(s) = 1$ could be as follows:

$$G_{OL}(s) = G_C(s)\cdot F_m(s)\cdot G_{PL}(s) = \\ = K_P \frac{\tau_{PI}\cdot s+1}{\tau_{PI}\cdot s}\cdot\frac{G_{PWM}}{1+\tau_{inv}s}\cdot\frac{k_{PL}}{1+\tau_{PL}\cdot s} \quad (14)$$

Where, a linear form of ***PWM Modulator TF*** could be a gain and the Control to IGBT-Bridge delay (less than 5 T_{pwm} times). Making use of the compensating terms (see equations (12) and (13)) *Plant TF* can be written as:

$$G_{PL}(s) = \frac{1}{R+L\cdot s} = \frac{k_{PL}}{1+\tau_{PL}\cdot s}, \quad (15)$$

$$\tau_{PL} = \frac{L}{R}; k_{PL} = \frac{1}{R}$$

PI regulator is calculated thanks to *Symmetry Criterion* [8], a system optimized by this technique shows overshoot of 43% under step change of the input signal. We have recalculated PI parameters forcing a damping factor of ξ =0.707 (overshoot less than 5%). Appling large time constant compensation τ_{PL} with PI zero ($\tau_{PI} = \tau_{PL}$), then:

$$G_{OL}(s) = K_P\frac{k_{PL}}{\tau_{PI}\cdot s}\cdot\frac{G_{PWM}}{1+\tau_{inv}s} = \frac{K_{OL}}{(1+\tau_{inv}s)\cdot(\tau_{PI}s)} \quad (16)$$

Where, $K_{OL} = K_P k_{PL} G_{PWM}$. Closed-Loop TF is:

$$G_{CL}(s) = \frac{G_{OL}(s)}{1+G_{OL}(s)} = \frac{\omega_n^2}{\omega_n^2 + 2\omega_n\xi s + s^2} \quad (17)$$

PI parameters are:

$$K_P = \frac{\tau_{PL}}{2\cdot\tau_{inv}\cdot k_{PL}\cdot G_{PWM}} \quad (18)$$

$$K_I = \frac{K_P}{\tau_{PI}} = \frac{1}{2\cdot\tau_{inv}\cdot k_{PL}\cdot G_{PWM}}$$

System Natural Frequency could be 3 or 5 times F_{PWM} (20KHz in this work):

$$\omega_n = \sqrt{\frac{K_P k_{PL} G_{PWM}}{\tau_{inv}\tau_{PL}}} \quad (19)$$

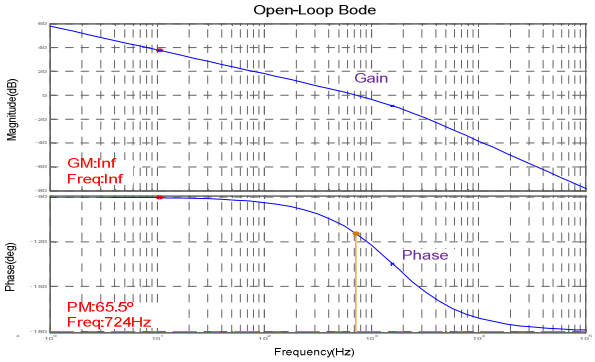

Fig. 4. Open-Loop Bode of GOL(s).

5. Resonant Control System, PR Controller.

Usually, current regulators for ac inverters are hysteresis controllers. The objective is to have zero phase and magnitude error thanks to the ac regulator. The principle is to find an equivalent ac compensation network with the same frequency response characteristic to the synchronous frame controller. Compensation terms are not needed because there aren't cross-coupling current terms. Figure 5 has the block abc/αβ which is implemented thanks to Scott Transform [2].

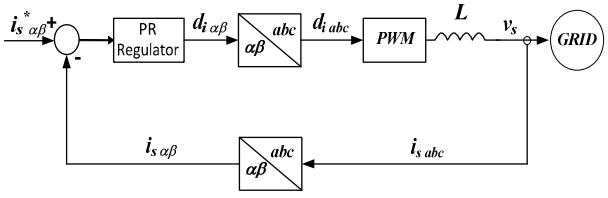

Fig. 5. Stationary Reference Frame Control scheme.

From this point, we need the transform that achieves this goal. When the reference signal bandwidth is small in comparison to the reference frequency itself we can use the transformation [5]:

$$H_{AC}(s) = H_{DC}\left(\frac{s^2+\omega_s^2}{2s}\right); \quad s \to \frac{s^2+\omega_s^2}{2s} \quad (20)$$

This variable transformation is developed in network synthesis to transform low-pass to band-pass filters. PI Integral Bode response seems to a low-pass filter and can be transformed by the use of (20). The new compensation network obtained is called *resonant regulator* or *P + Resonant system* (*PR*).

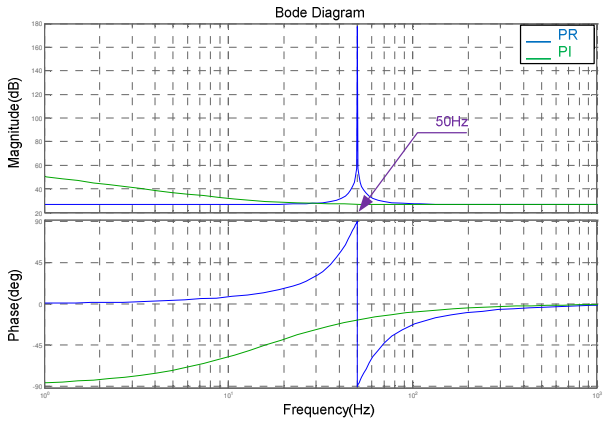

Fig. 6. Open Loop Bode plots of Stationary (blue) and Synchronous (green) Reference Frame.

With the PR we are working at the stationary frame, so we don't have the complexity of transforming a measured stationary frame ac current to rotating frame dc quantities. We can improve system response because we don't have rotating transformations errors. On the other hand, system resonance frequency is equal to the grid frequency with a gain up to 170dB. Note that Open Loop with PR control has a gain of 50dB at 49Hz and 51Hz, which are the European normative maximum deviation frequencies.

6. Simulation Results.

The control scheme has been simulated on Matlab Simulink® and its toolbox SimPowerSys. Table 1 is a summary of the system parameter values.

TABLE I. – Simulation Parameters

Parameter	Description	Value
L	Inductor filter	6mH
R	Inductor resistance	400mΩ
F_{PWM}	PWM carrier Frequency	20KHz
f	Grid frequency	50±1Hz
Sb	Base Power	3000VA
Vb	Line-to-Line RMS Base Voltage	400V
Vdc	DC Bus Voltage	750V
Kp	Proportional constant	30
Ki	Integral constant	2000

Source power is an ideal DC voltage source. Reference system power is unity step at 50ms from the start of simulation.

Figure 7 represents the VOC control scheme for the simulation in Simulink®. Output current needed for the Coupling terms is passed to blocks d_control and q_control through a "goto" signal routing.

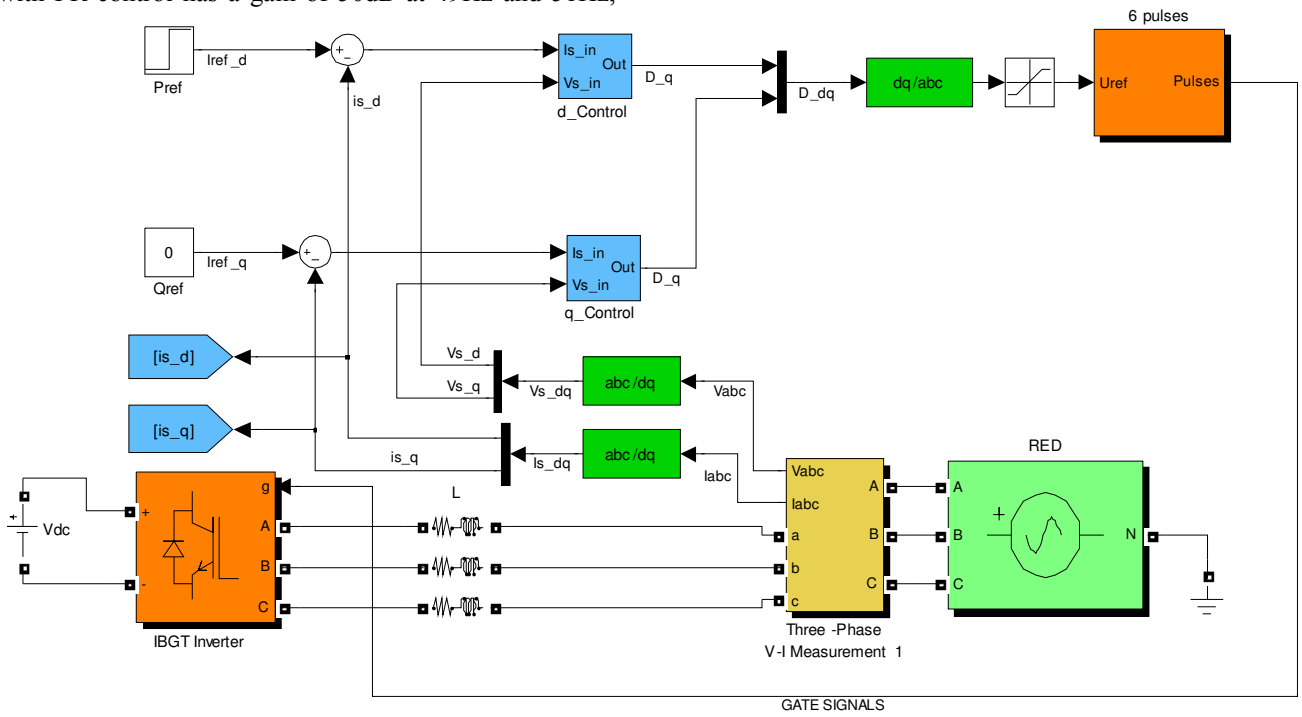

Fig. 7. Inverter Control Scheme for VOC control.

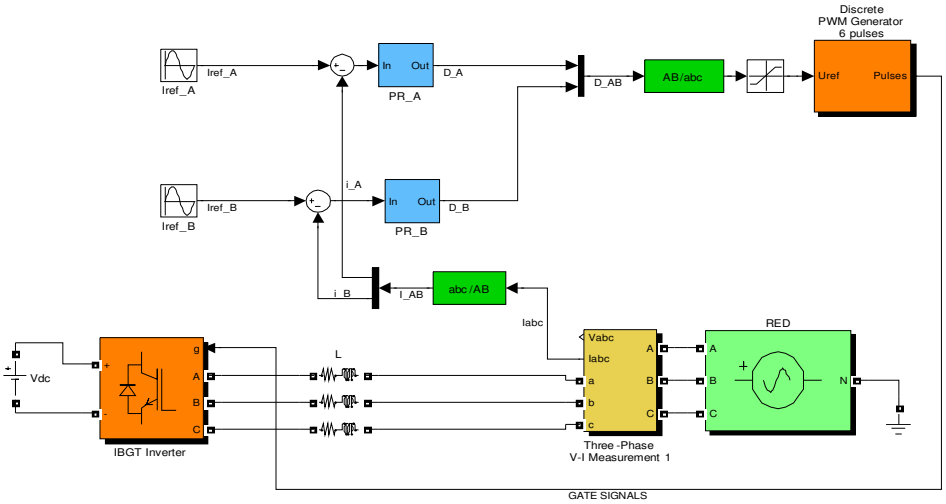

Fig. 8. Inverter scheme for Stationary Reference Frame Control.

Figure 8 represents the Stationary Reference Frame Control scheme for the simulation in Simulink®.

We introduce a grid-voltages variation of ±10% (see Figure 9). We define three intervals of interest, first interval is from 100ms to 300ms with 1pu voltages, second interval is from 300ms to 600ms with 1.1pu voltages, and third interval is from 600ms to 900ms with 0.9pu voltages.

From start to 300ms grid voltages are at rated value (1pu). Figure 11 shows *phase a* current and we can see the spectral content in Figure 12. This simulation results are for the VOC control without compensation terms. We have a Setting Time less than 350μs and no overshoot (Figure 10). This control achieves a good THD_i (FFT calculated over a running window of one fundamental cycle and Sample Frequency 1MHz) of 2.85%. This simulation results validate the calculated PI parameters.

Now, we want to compare VOC control with and without compensating terms. After that, VOC best results will be compared with the PR controller at the stationary frame.

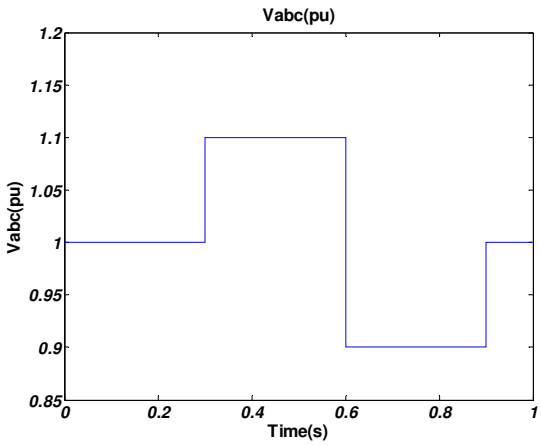

Fig. 9. Grid Voltages variation intervals in per unit quantities.

Figure 13 and Figure 14 presents *phase a* current and its spectrum in the second interval of time (from 300ms to 600ms), where the grid voltages are 1.1pu.

Figure 15 and Figure 16 presents *phase a* current and its spectrum in the third interval of time (from 600ms to 900ms), where the grid voltages are 0.9pu. Average THDi in second interval is 2.89%. This is the three interval worst THD_i and it is motivated by the loose of gain of the PWM modulator. At the third interval *phase a* current has a similar wave form that second interval with an interval average THD_i of 2.71%.

We follow with a VOC simulation with compensating terms. Results with VOC strategy with compensating could be seen from Figure 17 to Figure 22. This control exhibits a slightly better harmonic content (reader must see THD_i values and compare it) than VOC without compensating terms.

Now, we are going to compare THDi results with PR control strategy. From Figure 23 to Figure 28 paper shows the *phase a* inverter current with PR control in first, second and third interval and its spectral content. This kind of control presents the best results in terms of THD_i and harmonic-by-harmonic in all intervals. If we take a look to the worst interval case (0.3s to 0.6s), the THD_i is equal to 2.41% (0.47% better than VOC) with the same dynamic parameters than VOC control (setting time and overshoot, see Figure 10 and Figure 29).

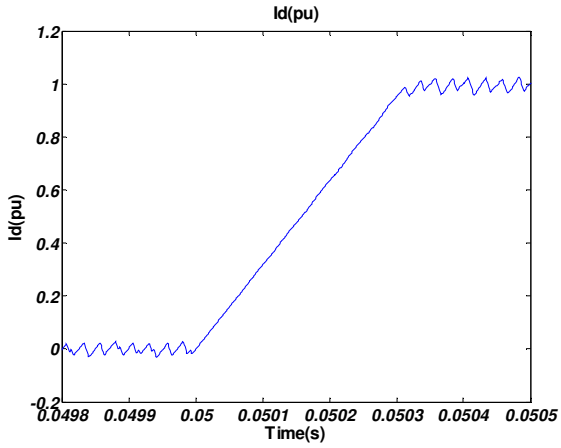

Fig. 10. Grid d-axis current with VOC control, setting time less that 350us and no overshoot.

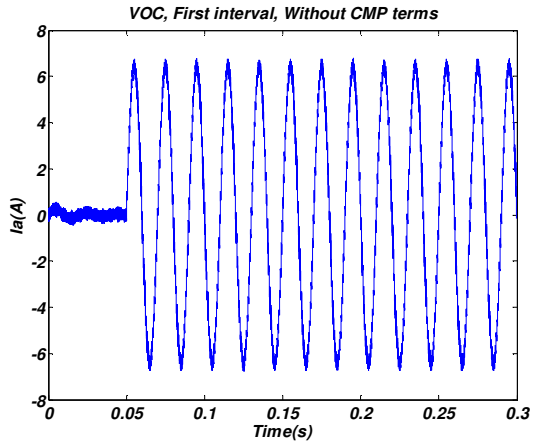

Fig. 11. Phase a current in the first interval of simulation without compensation terms.

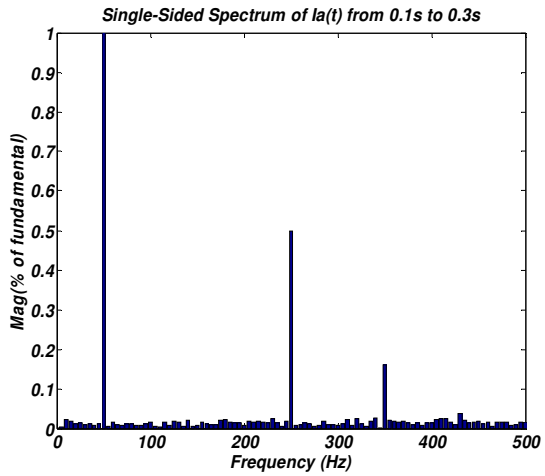

Fig. 12. Spectrum of Ia current from 0.1 to 0.3s, interval average THDi =2.85%.

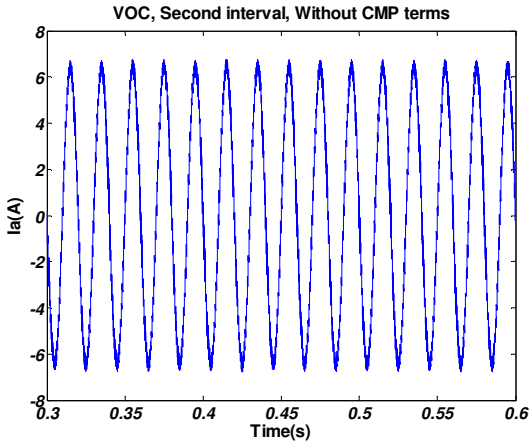

Fig. 13. Phase a current wave form in the second interval of simulation without compensation terms.

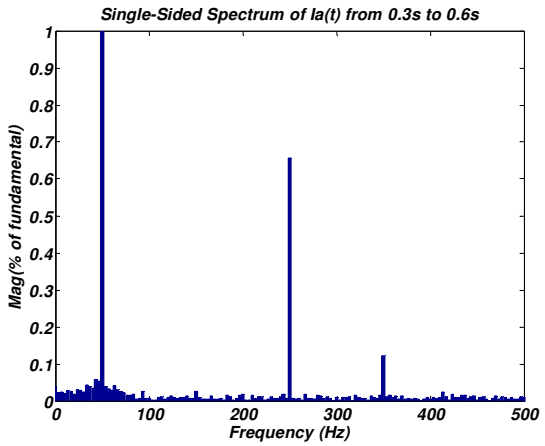

Fig. 14. Spectrum of Ia current from 0.3 to 0.6s, interval average THDi =2.89%.

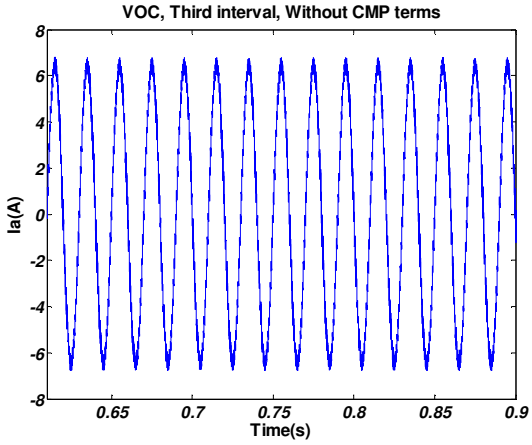

Fig. 15. Phase a current wave form in the third interval of simulation without compensation terms.

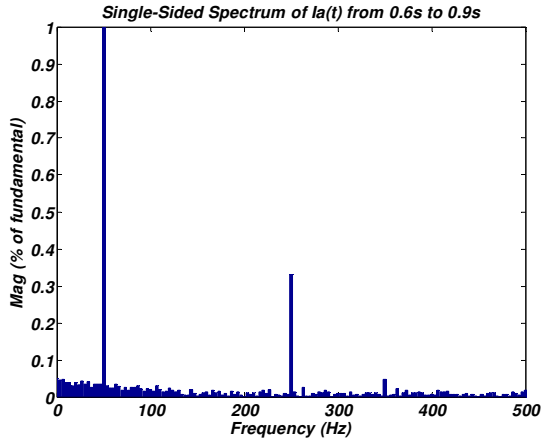

Fig. 16. Spectrum of Ia current from 0.6 to 0.9s, interval average THDi =2.71%.

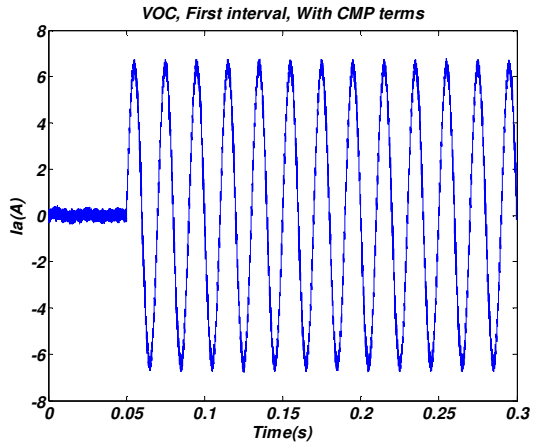

Fig. 17. Phase a current wave form in the first interval of simulation with compensation terms.

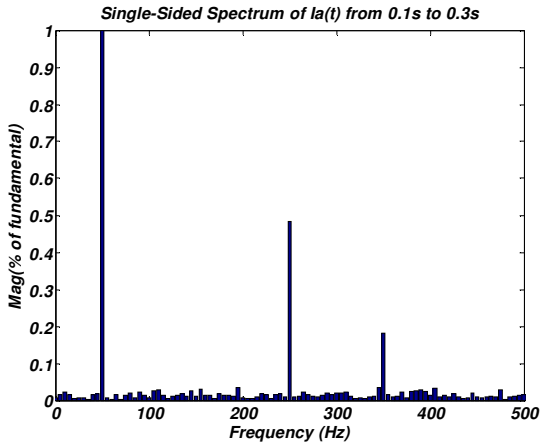

Fig. 18. Spectrum of Ia current from 0.1 to 0.3s, interval average THDi =2.84%.

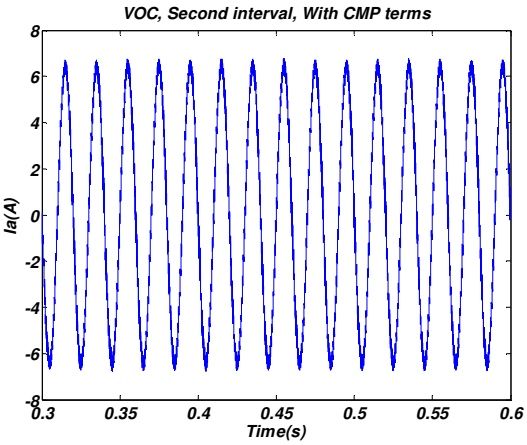

Fig. 19. Phase a current wave form in the second interval of simulation with compensation terms.

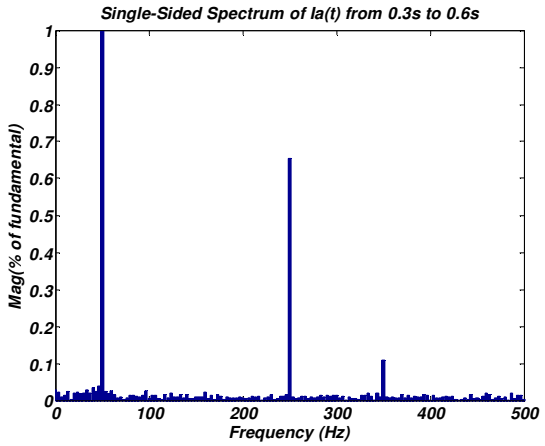

Fig. 20. Spectrum of Ia current from 0.3 to 0.6s, interval average THDi =2.88%.

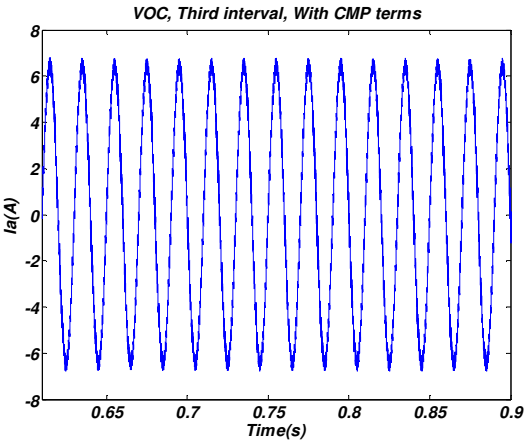

Fig. 21. Phase a current wave form in the third interval of simulation with compensation terms.

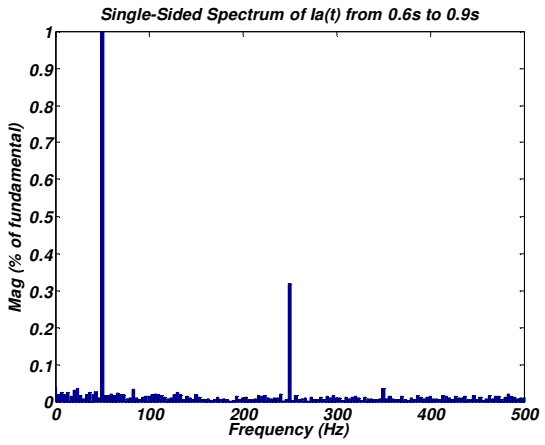

Fig. 22. Spectrum of Ia current from 0.6 to 0.9s, interval average THDi =2.70%.

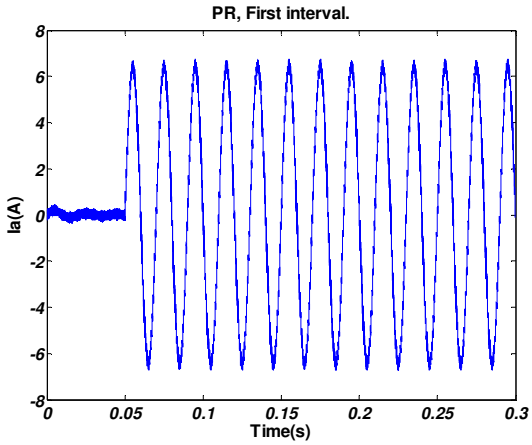

Fig. 23. Phase a current wave form in the first interval of simulation with PR control.

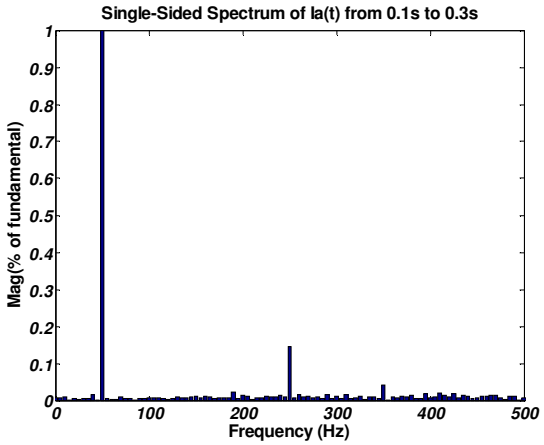

Fig. 24. Spectrum of Ia current from 0.6 to 0.9s, interval average THDi =2.31%.

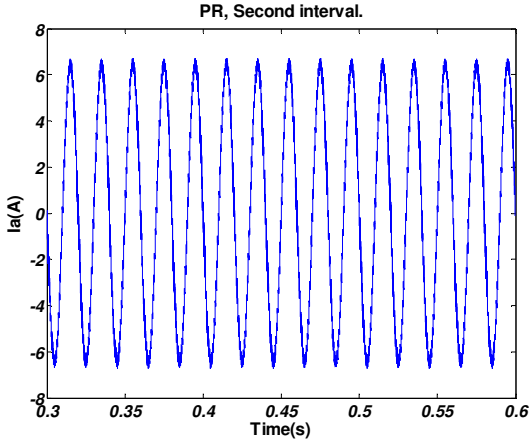

Fig. 25. Phase a current wave form in the first interval of simulation with PR control.

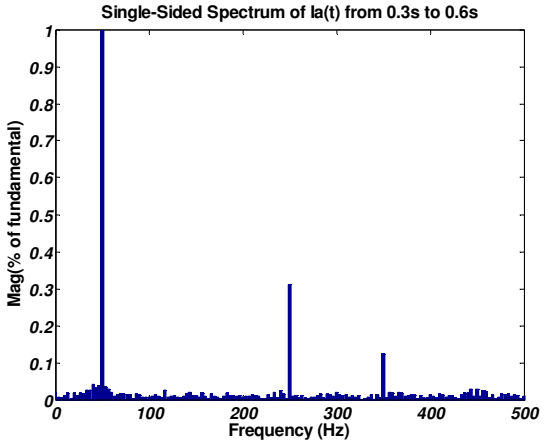

Fig. 26. Spectrum of Ia current from 0.6 to 0.9s, interval average THDi =2.41%.

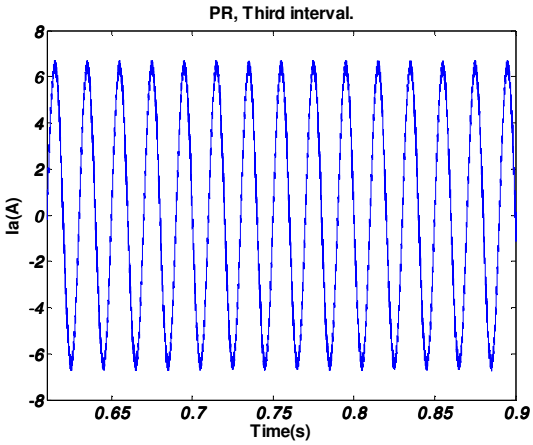

Fig. 27. Phase a current wave form in the third interval of simulation with PR control.

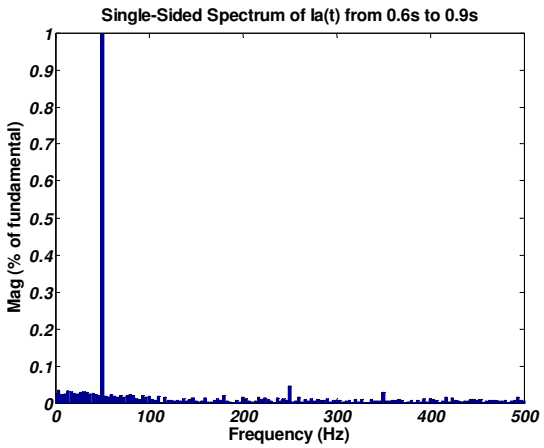

Fig. 28. Spectrum of Ia current from 0.6 to 0.9s, interval average THDi =2.19%.

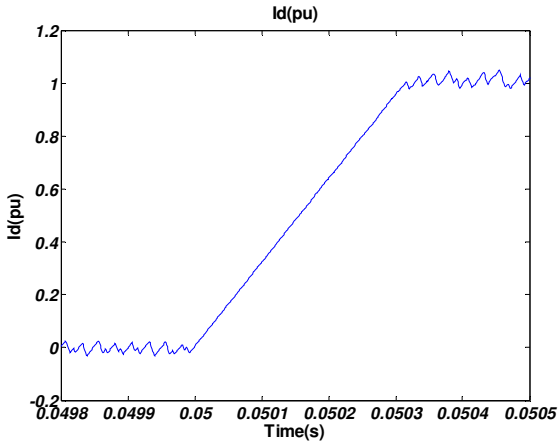

Fig. 29. Grid d-axis current with PR control. Setting Time less that 350us and no overshoot.

7. Conclusion

This Paper presents a comparison of the *Synchronous Reference Frame* (*VOC* applied to grid voltage*)* and *Stationary Reference Frame* control strategies used in VSI current mode control.

Paper starts providing background on the grid model and *VOC PI regulator* parameters are obtained with a modified *Symmetry Criterion* method. From this point we transform the PI regulator into a *Proportional-Resonant* controller which will be used in the Stationary Reference Frame.

Control strategies proposed has less harmonic content at third interval of simulation (600ms to 900ms) when grid voltages are 0.9pu. This is motivated by the bigger system PWM gain than first and second intervals. With a High Gain PWM system can follow the control current references better.

Simulation results shown in terms of THD_i, indicate that PR control improves THD_i with the same dynamic characteristics of VOC control. At the worst case (second interval) PR control presents an interval average THD_i of 2.41%, meanwhile VOC has 2.88% at the same interval with compensating terms strategy. The relative improvement is up to 16%. It's known that Stationary Frame control needs less mathematical calculus than a Voltage Oriented Control. PR control is a good alternative to implement an inverter system control with reduced harmonic content injected into the grid and less computational load than VOC control.

Acknowledgement

This work is supported in part by "PROYECTO SINGULAR ESTRATÉGICO EN MINIEÓLICA PSE-MINIEOLICA" reference FIT-120000-2007-245 and Bornay Aerogeneradores S.U. (Comunidad Valenciana – SPAIN) in collaboration with the Politechnic University of Valencia.

References

[1] A.J.G. Westlake, J.R. Bumby and E. Spooner, "Damping the power-angle oscillations of a permanent-magnet synchronous generator with particular reference to wind turbine applications" IEE Proc.-Electr. Power Appl., vol. 143,no3, pp269-280, May, 1996.

[2] Adil M. Al-Zamil, David A. Torrey, "A passive Series, Active Shunt filter for High Power Applications" IEEE TRANSACTIONS ON POWER ELECTRONICS, VOL 16, NO.1, JANUARY 2001.

[3] Soares dos Reis, F.; Ale, J.A.V.; Adegas, F.D.; Tonkoski, R.; Slan, S.; Tan, K.;" Active Shunt Filter for Harmonic Mitigation in Wind Turbines Generators" Power Electronics Specialists Conference, 2006. PESC '06. 37th IEEE.

[4] G. Giglia, M. Pucci, C. Serporta, G. Vitale, "Comparison of Control Techniques for Three-Phase Distributed Generation Based on VOC an DPC" ICREPQ 2008.

[5] Daniel Nahum Zmood, Donald Grahame Holmes. "Stationary Frame Current Regulation of PWM Inverters With Zero Steady-State Error" IEEE Transactions On Power Electronics, Vol.18, No.3, May 2003.

[6] Said El-Barbari, W. Hofmann, "Digital Control of a Three Phase 4 Wire PWM Inverter for PV Applications" EPE'99-Lausanne.

[7] Timothy M. Wowan, Russel J. Kerkman Thomas A. Lipo, "Operation of PWM Voltage Source-Inverters in the Overmodulation Region" IEEE TRANSACTIONS ON INDUSTRY APPLICATIONS, VOL 43, NO. 1, FEBRUARY 1996.

[8] M.P. Kazmierkowski, "Automatic Control of Converter-Fed Drives" The Netherlands, Elsevier, 1994.

[9] M.H. Rashid, "Power Electronics Handbook" Academic Press, 2001.